THE JOURNAL OF BIOLOGICAL CHEMISTRY
Vol. 280, No. 18, Issue of May 6, pp. 18008–18014, 2005

Printed in U.S.A.

Mg^{2+} and Ca^{2+} Differentially Regulate DNA Binding and Dimerization of DREAM*

Received for publication, January 11, 2005, and in revised form, February 22, 2005
Published, JBC Papers in Press, March 3, 2005, DOI 10.1074/jbc.M500338200

Masanori Osawa‡§, Alexandra Dace‡, Kit I. Tong¶, Aswani Valiveti‡, Mitsuhiko Ikura¶, and James B. Ames‡‖

From the ‡Center for Advanced Research in Biotechnology, University of Maryland Biotechnology Institute, Rockville, Maryland 20850 and the ¶Division of Molecular and Structural Biology, Ontario Cancer Institute and Department of Medical Biophysics, University of Toronto, Ontario M5G 2M9, Canada

DREAM (calsenilin/KChIP3) is an EF-hand calcium-binding protein that represses transcription of prodynorphin and c-*fos* genes. Here we present structural and binding studies on single-site mutants of DREAM designed to disable Ca^{2+} binding to each of the functional EF-hands (EF-2: D150N; EF-3: E186Q; and EF-4: E234Q). Isothermal titration calorimetry (ITC) analysis of Ca^{2+} binding to the various mutants revealed that, in the absence of Mg^{2+}, Ca^{2+} binds independently and sequentially to EF-3 ($\Delta H = -2.4$ kcal/mol), EF-4 ($\Delta H = +5.2$ kcal/mol), and EF-2 ($\Delta H = +1$ kcal/mol). By contrast, only two Ca^{2+} bind to DREAM in the presence of physiological levels of Mg^{2+} for both wild-type and D150N, suggesting that EF-2 binds constitutively to Mg^{2+}. ITC measurements demonstrate that one Mg^{2+} binds enthalpically with high affinity ($K_d = 13\ \mu M$ and $\Delta H = -0.79$ kcal/mol) and two or more Mg^{2+} bind entropically in the millimolar range. Size-exclusion chromatography studies revealed that Mg^{2+} stabilizes DREAM as a monomer, whereas Ca^{2+} induces protein dimerization. Electrophoretic mobility shift assays indicated that Mg^{2+} is essential for sequence-specific binding of DREAM to DNA response elements (DREs) in prodynorphin and c-*fos* genes. The EF-hand mutants bind specifically to DRE, suggesting they are functionally intact. None of the EF-hand mutants bind DRE at saturating Ca^{2+} levels, suggesting that binding of a single Ca^{2+} at either EF-3 or EF-4 is sufficient to drive conformational changes that abolish DNA binding. NMR structural analysis indicates that metal-free DREAM adopts a folded yet flexible molten globule-like structure. Both Ca^{2+} and Mg^{2+} induce distinct conformational changes, which stabilize tertiary structure of DREAM. We propose that Mg^{2+} binding at EF-2 may structurally bridge DREAM to DNA targets and that Ca^{2+}-induced protein dimerization disrupts DNA binding.

DREAM[1] (downstream regulatory element antagonist modulator also known as calsenilin (1) and KChIP3 (2)) is a 29-kDa EF-hand Ca^{2+}-binding protein that serves as a transcriptional repressor for pain modulation (3–5). DREAM translocates into the nucleus during calcium signaling (6) and blocks transcription of prodynorphin and c-*fos* genes by binding to specific DNA sequences (DRE, downstream regulatory element (7, 8)) in a Ca^{2+}-dependent fashion (9–11). The importance of DREAM as a calcium-sensitive transcriptional repressor has been demonstrated in DREAM-deficient mice that exhibit the very striking phenotype of ongoing analgesia due to up-regulated expression of prodynorphin (12, 13). The DREAM knock-out mice also exhibit mild effects on β-amyloid production and long-term potentiation (13), but do not exhibit any motor or behavioral abnormalities. Hence, DREAM regulates pain transmission by controlling prodynorphin expression and represents an attractive therapeutic opportunity for managing pain.

DREAM contains four EF-hands similar to the Ca^{2+}-binding motifs found in calmodulin and troponin C (14, 15). The four EF-hands of DREAM are >45% identical in sequence to recoverin and related Ca^{2+} sensors of the neuronal calcium sensor (NCS) subclass of the EF-hand superfamily (16, 17) (see Fig. 1). A characteristic feature of DREAM and the NCS family is the sequence CP*X*G (Cys-104 and Pro-105, see Fig. 1) that prevents the binding of Ca^{2+} to the first EF-hand (EF-1) as seen in the crystal structures of recoverin (18), KChIP1 (19, 20), neurocalcin (21), and frequenin (22). The second EF-hand (EF-2) of DREAM contains aspartate (Asp-150) instead of the usual glutamate at the 12-position of the EF-hand binding loop (Fig. 1). The presence of aspartate at the 12-position in other EF-hand proteins is known to diminish its binding selectivity of Ca^{2+} *versus* Mg^{2+} (23). Mg^{2+} binding to the second EF-hand of DREAM might be sufficient to affect DREAM structure and DNA binding. Indeed, a recent mass spectrometry study revealed that both Ca^{2+} and Mg^{2+} are bound by DREAM (24). Magnesium is not normally considered a regulator, but recent *in vivo* measurements have detected changes in free Mg^{2+} concentrations in cortical neurons after treatment with neurotransmitter (25). Other NCS proteins such as GCAPs, VILIP, and NCS-1 also bind Mg^{2+} and exhibit Mg^{2+}-induced effects (26, 27). Therefore, it is of interest to investigate the functional role of Mg^{2+} binding to DREAM and determine whether Mg^{2+} might control the binding of DREAM to DNA targets.

Here, we present a structural analysis of Mg^{2+} and Ca^{2+}

* This work was supported in part by a Beckman Foundation Young Investigator Award (to J. B. A.) and Grants NS45909 and EY12347 from the National Institutes of Health (to J. B. A). The costs of publication of this article were defrayed in part by the payment of page charges. This article must therefore be hereby marked "*advertisement*" in accordance with 18 U.S.C. Section 1734 solely to indicate this fact.

§ Supported by postdoctoral fellowships from the Human Frontier Science Program and Uehara Memorial Foundation.

‖ To whom correspondence should be addressed: The Center for Advanced Research in Biotechnology, University of Maryland Biotechnology Institute, 9600 Gudelsky Dr., Rockville, MD 20850. Tel.: 301-738-6120; Fax: 301-738-6255; E-mail: james@carb.nist.gov.

[1] The abbreviations used are: DREAM, downstream regulatory element antagonist modulator; DREAM-C, deletion mutant of mouse DREAM consisting of residues 65–256; apoDREAM-C, metal-free DREAM; Mg^{2+}-DREAM-C, Mg^{2+}-bound DREAM; Ca^{2+}-DREAM-C, Ca^{2+}-bound DREAM; HSQC, heteronuclear single quantum coherence; ITC, isothermal titration calorimetry; KChIP, potassium channel-interacting protein; SEC, size exclusion chromatography; EMSA, electrophoretic mobility-shift analysis; NOE, nuclear Overhauser effect; NOESY, NOE spectroscopy.

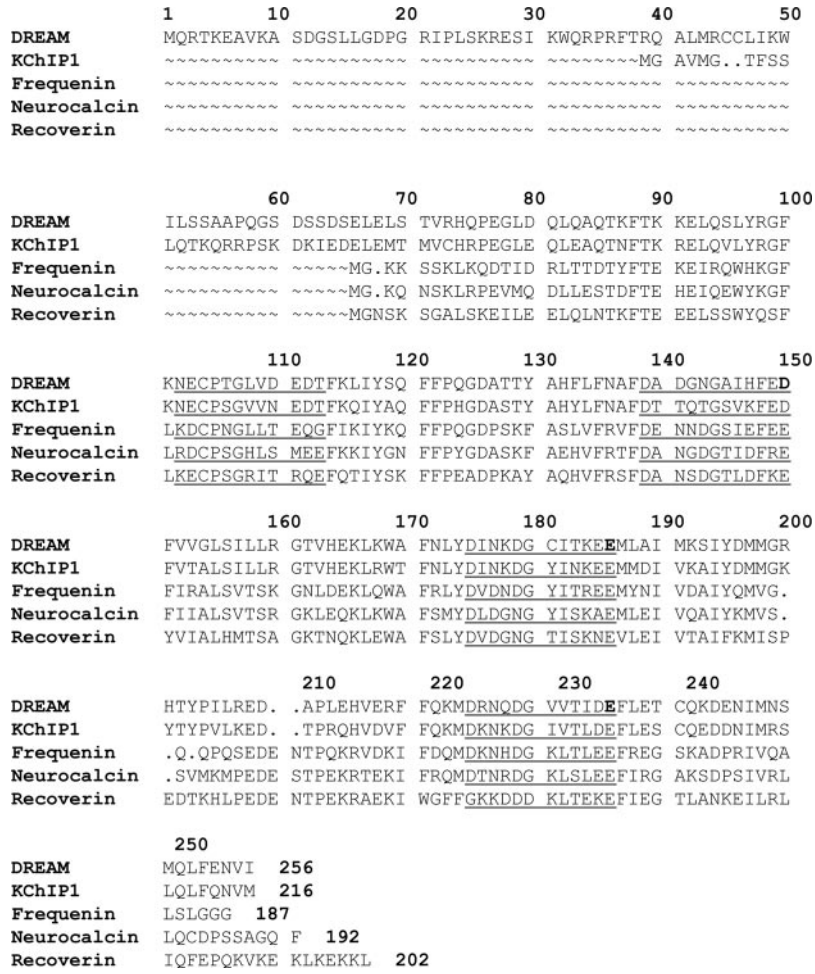

FIG. 1. **Alignment of amino acid sequence of mouse DREAM with various members of the recoverin branch of the EF-hand superfamily.** The Ca^{2+} binding loops of the four EF-hands are *underlined*. A negatively charged residue at the 12-position of the functional EF-hand loops (Glu or Asp in *bold*) were individually mutated to the corresponding neutral residue (Gln or Asn) to disable functional Ca^{2+} binding to the respective EF-hands.

binding to the individual EF-hands in DREAM. The results reveal that Mg^{2+} is required for sequence-specific DNA binding; Mg^{2+} binds constitutively at EF-2; Mg^{2+} stabilizes a monomeric form of DREAM; Ca^{2+} induces protein dimerization; and Ca^{2+} binding at either EF-3 or EF-4 is sufficient to abolish DNA binding at high Ca^{2+}. On the basis of these results, a structural model for Ca^{2+}-sensitive DNA binding by DREAM will be presented.

EXPERIMENTAL PROCEDURES

Expression and Purification of Mouse DREAM-C and Its Mutants—A deletion mutant of mouse DREAM (residues 65–256, named DREAM-C) was shown previously to exhibit functional binding to DNA and Ca^{2+} (10). The recombinant DREAM-C protein was expressed in soluble form and could be purified in milligram amounts, in contrast to the recombinant full-length protein, which appeared insoluble in bacterial extracts. Gene sequences encoding wild-type DREAM-C and its mutants D150N, E186Q, and E234Q were inserted into pET15b (Novagen) expression vectors. These constructs were transformed into *Escherichia coli* BL21(DE3) (Stratagene) cells and were grown in 2 liters of LB medium with 100 μg/ml ampicillin at 37 °C. Recombinant DREAM-C protein expression was induced by adding 0.5 mM isopropyl 1-thio-β-D-galactopyranoside to the cell culture once the cell culture reached an optical density of 0.5 at 600 nm, and the cells were then grown with shaking at 37 °C for 3 h or 16 °C overnight. Cells were harvested by centrifugation and resuspended in buffer A (20 mM Tris·HCl, pH 8.0, 0.3 M NaCl, 1 mM β-mercaptoethanol, and 20% glycerol) supplemented with 1 mM phenylmethylsulfonyl fluoride, 0.2% Tween 20, 20 μg/ml DNase I, and 5 mM $MgCl_2$. Cells were then disrupted by sonication, and soluble protein fractions recovered by centrifugation were applied onto a nickel-loaded Hi-Trap chelating column on an ΔKTA purifier (Amersham Biosciences), previously equilibrated with buffer A. After washing with the buffer A (until $A_{280} < 0.01$), proteins were eluted with buffer A containing 0.3 M imidazole. The eluted solution was dialyzed *versus* buffer B (10 mM Tris·HCl, pH 7.4, 1 mM EDTA, and 1 mM dithiothreitol) for 12 h. The dialyzed sample was applied onto a Hi-Trap DEAE-FF column (Amersham Biosciences) previously equilibrated in the buffer B, and eluted with NaCl gradient (0 to 0.3 M NaCl over 3 h) at a flow rate of 5 ml/min.

Size Exclusion Chromatography—Determination of the molecular weight of the purified DREAM-C in solution was carried out on a Superdex 200 HR 10/30 column (Amersham Biosciences) at 4 °C in the buffers containing 10 mM Tris-HCl (pH 7.6), 150 mM NaCl, 5 mM $MgCl_2$, 1 mM dithiothreitol, and 5 mM $CaCl_2$ for Ca^{2+}-DREAM-C, or 1 mM EGTA for Mg^{2+}-bound DREAM-C. 0.1 ml of DREAM-C (protein concentration ranged from 10 to 460 μM) was loaded onto the column and eluted at a flow rate of 0.5 ml/min. Apparent molecular weights were calculated using a standard curve of V_e/V_o *versus* the log of the molecular masses of standard proteins: β-amylase (200 kDa), alcohol dehydrogenase (150 kDa), transferrin (81 kDa), carbonic anhydrase (29 kDa), and myoglobin (17 kDa). V_o is a void volume obtained using blue dextran (2000 kDa), and V_e is a volume of elution.

Preparation of Decalcified Protein Solutions—Decalcified ITC buffer (150 mM NaCl and 10 mM Tris-HCl, pH 7.6) was prepared by treatment with Chelex 100 resin (Bio-Rad). 1 mM dithiothreitol and 5 mM $MgCl_2$ were added after treatment with Chelex 100 and immediately before use. Containers and pipette tips were rinsed with 1 M HCl twice followed by a rinse with decalcified buffer. EDTA was removed from protein solution using Econo-Pac 10 DG gel filtration column (Bio-Rad Laboratories, Inc.) pre-equilibrated in the decalcified buffer. Before the ITC experiment, the sample cell and injection syringe of ITC machine (Microcal Inc.) was cleaned by the decalcified buffer extensively.

Mg^{2+} and Ca^{2+} Titration into DREAM-C by ITC—Binding of Mg^{2+} and Ca^{2+} to DREAM-C was measured by ITC (28) using a MicroCal VP-ITC MicroCalorimeter (MicroCal Inc.). The protein solution used in the titration was exchanged with decalcified buffer using Econo-Pac 10 desalting gel-filtration column as described above. Stock solutions of $MgCl_2$ and $CaCl_2$ (0.5–2.0 mM), used as the titrant, were prepared using decalcified buffer as a diluent. A stock solution of $CaCl_2$ with 5 mM $MgCl_2$ was the titrant for Ca^{2+} titration of Mg^{2+}-bound DREAM-C. A typical ITC experiment was performed at 25 °C on a protein solution

(1.38 ml, 35–100 μM) by adding a total of 290 μl of concentrated $MgCl_2$ or $CaCl_2$ (0.50–2.0 mM) in 29 aliquots (10 μl each). The additions were 3 min apart to allow heat accompanying each increment to return to baseline prior to the next addition. For each addition, the molar heat (Q_t) was measured as a function of total ligand concentration (X_t),

$$Q_t = n*M_t*\Delta H*V\{1 + X_t/(n*M_t) + 1/(n*K_a*M_t) - [(1 + X_t/(n*M_t) + 1/(n*K_a*M_t)^2 - 4X_t/(n*M_t)]^{0.5}\}/2 \quad \text{(Eq. 1)}$$

where n is the number of sites, M_t is the total protein monomer concentration, K_a is the metal-binding association constant ($1/K_d$), and V is the cell volume. The differential molar heat (dQ_t) measured in the ITC experiment was fit to various kinetic models (sequential *versus* independent sites) using a nonlinear least squares minimization method (28, 29). Thermodynamic parameters in the analysis are defined by,

$$\Delta G = \Delta H - T\Delta S \quad \text{(Eq. 2)}$$

and

$$\Delta G = -nRT \ln(K_a) \quad \text{(Eq. 3)}$$

where n is the number of moles, T is the absolute temperature, and R = 8.3151 J mol^{-1} K^{-1}.

NMR Spectroscopy—Samples for NMR analysis were prepared by dissolving ^{15}N-labeled DREAM-C (0.2–0.5 mM) in 0.3 ml of a 95% H_2O/5% [^2H]H_2O solution containing 10 mM [$^2H_{11}$]Tris (pH 7.4), 5 mM [$^2H_{10}$]dithiothreitol, 50 mM KCl, and either 5 mM EDTA (apo), 5 mM $MgCl_2$ (Mg^{2+}-bound), or 5 mM $CaCl_2$ plus 5 mM $MgCl_2$ (Mg^{2+}/Ca^{2+}-bound). All NMR experiments were performed at 32 °C on a Bruker Avance 600-MHz spectrometer equipped with a four-channel interface and triple-resonance probe with triple-axis pulsed field gradients. The ^{15}N-^1H HSQC spectra (see Fig. 6) were recorded on samples of ^{15}N-labeled DREAM-C (in 95% H_2O, 5% ^2H_2O). The number of complex points and acquisition times were: 256, 180 ms (^{15}N (F_1)), and 512, 64 ms (^1H (F_2)).

Fluorescent EMSA—Synthetic oligonucleotides (purchased from ACGT Corp., Toronto, Canada) representing the DRE of human prodynorphin (9, 10) were 5′-labeled using the fluorescent dye, Cy5 (Amersham Biosciences). The precise nucleotide sequence was 5′-GAAGCCGGAGTCAAGGAGGCCCCTG-3′. Complementary strands were denatured at 95 °C for 10 min and annealed by slowly cooling to room temperature in the presence of 20 mM Tris-HCl, pH 7.6, 10 mM $MgCl_2$, and 0.1 mM EDTA. Formation of double-stranded DNA was checked on a 20% non-denaturing polyacrylamide/0.25 × TBE/1%glycerol gel prior to binding.

DREAM-C proteins (wild-type, D150N, E186Q, and E234Q) were exchanged firstly to 20 mM Tris-HCl, pH 7.4, 10% glycerol, 100 mM NaCl, 5 mM dithiothreitol, 0.5 mM EDTA using PD-10 columns and concentrated by Centricon 10 (Millipore) at 4 °C. Protein (0–70 μM, Fig. 7) was then incubated with 5 nM Cy5-labeled duplex DNA for 5 h at room temperature in 10 mM HEPES, pH 7.9, 8 mM $MgCl_2$, 0.1 mM EDTA, 2 mM dithiothreitol, 1 nM (0.05 unit/ml) of poly(dI-dC) (Amersham Biosciences), and with or without 10 mM $CaCl_2$. Protein·DNA complexes were resolved in 5% non-denaturing polyacrylamide/0.25 × TBE/1% glycerol gels at 200 V for 30 min in 0.25 × TBE and 0.5 mM $MgCl_2$ running buffer. Wet fluorescent gels were scanned using the red fluorescence mode of a Storm 860 system (Amersham Biosciences) with a voltage setting of 1000 V and a scanning resolution of 200 μM.

RESULTS AND DISCUSSION

ApoDREAM-C Binds Three Ca^{2+} Ions—Isothermal titration calorimetry (ITC, see Equations 1–3) was used in this study to analyze the energetics of Ca^{2+} and Mg^{2+} binding to the individual EF-hands of DREAM-C. Intrinsic metal binding to proteins is usually entropically driven ($\Delta H > 0$) due to very high dehydration energies of divalent cations. However, the enthalpy of binding can become exothermic ($\Delta H < 0$) if metal binding is coupled to a protein conformational change (30).

The Ca^{2+} binding properties of metal-free DREAM-C (apoDREAM-C) were monitored by ITC (Fig. 2). Titration of $CaCl_2$ into apoDREAM-C (in the absence of Mg^{2+}) resulted in a binding isotherm that is multiphasic and could be fit by the binding of three or more Ca^{2+} ions, consistent with previous binding studies (10, 24). The isotherm exhibited stoichiometric binding of two Ca^{2+} ($K_d \sim$ 1–10 μM) followed by endothermic binding of one or more Ca^{2+} ion(s) with much lower affinity. The binding isotherm is too complex to accurately quantitate the thermodynamic properties of each of the binding sites. To simplify the analysis, we have constructed various single-site mutants that disable functional Ca^{2+} binding to the individual EF-hands (Fig. 1): D150N (EF-2), E186Q (EF-3), and E234Q (EF-4). In each mutant, a negatively charged Glu or Asp at the 12-position in the EF-hand loop has been substituted with a corresponding neutral residue (Gln or Asn) that dramatically lowers the Ca^{2+} binding affinity of the respective EF-hand outside of the physiological range of Ca^{2+} (31, 32).

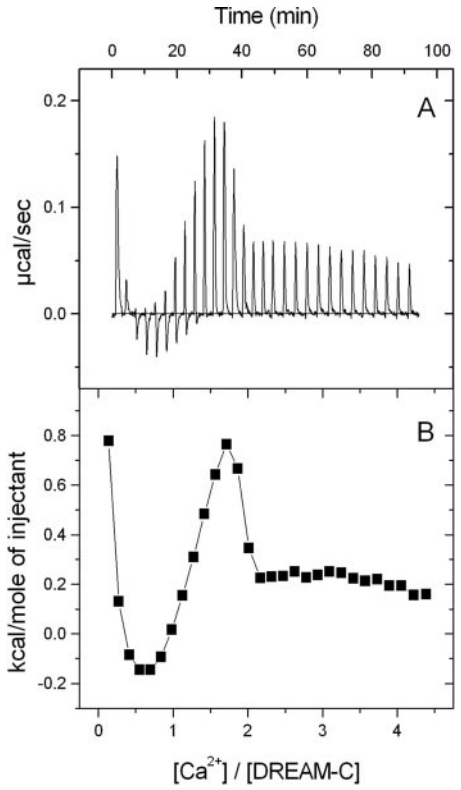

FIG. 2. **Isothermal titration microcalorimetric analysis of Ca^{2+} binding to apoDREAM-C.** Trace of the calorimetric titration of 29 × 10-μl aliquots of 1.3 mM $CaCl_2$ into the cell containing 46 μM apoDREAM-C (*A*), and integrated binding isotherm (*B*). No correction was needed for the heat of dilution, because negligible heat was observed when adding aliquots of $CaCl_2$ (or $MgCl_2$) into a decalcified buffer blank.

An overlay of the Ca^{2+}-binding isotherms for each of the EF-hand mutants is shown in Fig. 3. The ITC isotherm of D150N exhibits stoichiometric binding of two Ca^{2+} ions but lacks the low affinity endothermic phase seen in wild-type, suggesting that EF-2 is the low affinity site. The isotherm of E186Q exhibits a strongly endothermic phase ($K_d \sim$ 1 μM and ΔH = +5.2 kcal/mol) assigned to Ca^{2+} binding at EF-4 and the low affinity phase assigned above to EF-2. The isotherm of E234Q exhibits an exothermic phase ($K_d \sim$ 1 μM and ΔH = −2.4 kcal/mol) assigned to Ca^{2+} binding at EF-3 and the low affinity phase assigned to EF-2. The exothermic Ca^{2+} binding to EF-3 and U-shaped isotherm suggest that a protein conformational change might accompany binding at EF-3.

In summary, EF-2 is an endothermic site with low affinity that gives rise to the non-stoichiometric binding in the wild-type isotherm. EF-3 and EF-4 are relatively high affinity sites (stoichiometric binding) whose enthalpies nearly cancel one another in the wild-type isotherm. A recent mass spectrometry analysis of DREAM suggested that a fourth Ca^{2+} might bind to DREAM at EF-1 (24), although the affinity of this site was not reported, and the binding of a fourth Ca^{2+} might be artificially

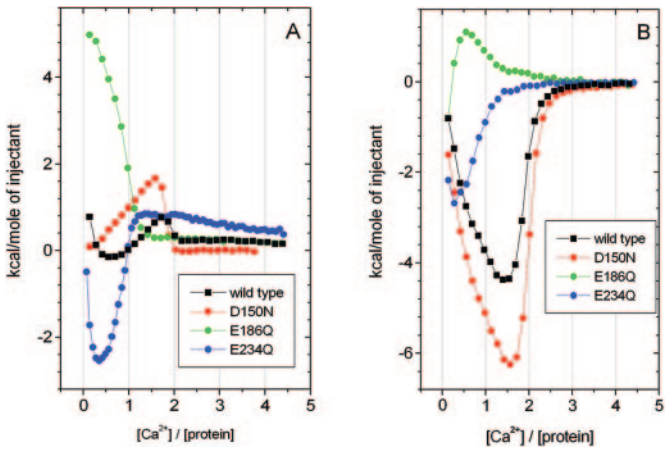

FIG. 3. **Comparison of Ca^{2+} binding isotherms for DREAM-C and EF-hand mutants (D150N, E186Q, and E234Q).** Ca^{2+} binding isotherms of apoDREAM-C (without $MgCl_2$) and Mg^{2+}-saturated protein (5 mM $MgCl_2$) are depicted in *A* and *B*, respectively. Wild-type DREAM-C, D150N, E186Q, and E234Q are shown in *black*, *red*, *green*, and *blue*, respectively. A *dotted line* in panel *B* shows the normalized sum of isotherms for E186Q and E234Q mutants.

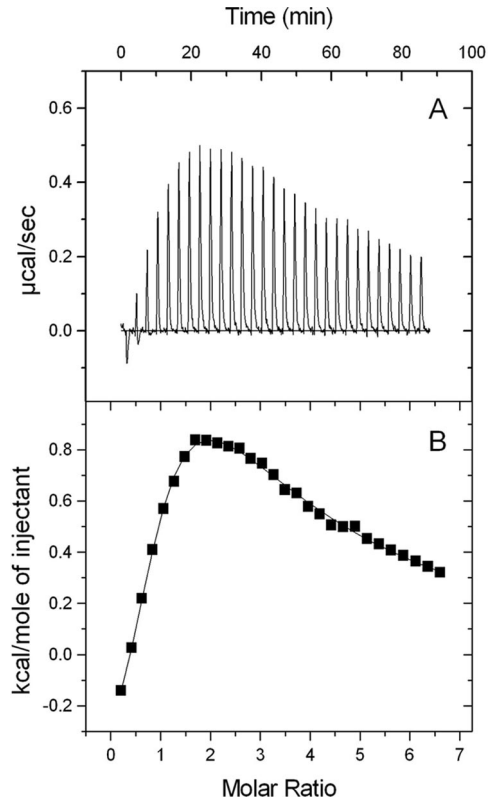

FIG. 4. **Isothermal titration microcalorimetric analysis of the Mg^{2+} binding to DREAM-C.** Trace of the calorimetric titration of 29 × 10-μl aliquots of 2.0 mM $MgCl_2$ into the cell containing 69 μM apoDREAM-C (*A*) and integrated binding isotherm (*B*). The binding isotherm in *B* was fit using a two-site model where $n_1 = 0.91 \pm 0.01$, $K_1 = (7.5 \pm 0.7) \times 10^4$ [M^{-1}], $\Delta H_1 = -791 \pm 90$ [cal·mol^{-1}]; $n_2 = 2$ (fixed), $K_2 = (4.3 \pm 0.2) \times 10^3$ [M^{-1}], $\Delta H_2 = (3.97 \pm 0.06) \times 10^3$ [cal·mol^{-1}].

enhanced in gas phase species analyzed in mass spectrometry experiments. The primary sequence of EF-1 contains unfavorable substitutions (*e.g.* Cys-104, Pro-105, and Thr-113) that would be expected to abolish physiological Ca^{2+} binding at this site as has been demonstrated in other NCS proteins (16, 18, 19). Accordingly, our ITC Ca^{2+} binding measurements performed on samples of DREAM-C in solution do not detect any Ca^{2+} binding at EF-1, suggesting that either EF-1 does not bind Ca^{2+} under physiological conditions or the enthalpy of binding is zero.

The wild-type Ca^{2+}-binding isotherm (in the absence of Mg^{2+}) is approximately represented as the normalized sum of isotherms for the three single-site mutants, implying three independent Ca^{2+}-binding sites. The Ca^{2+} binding also appears ordered. We suggest that Ca^{2+} binds to EF-3 first, because the beginning of the wild-type isotherm (0 to 1 equivalents) resembles that of E186Q. A second Ca^{2+} binds subsequently at EF-4, because the middle of the wild-type isotherm (from 1 to 2 equivalents) resembles that of E234Q. Lastly, a third Ca^{2+} binds to apoDREAM-C at EF-2, because the low affinity phase (beyond 2 equivalents) is abolished in the D150N isotherm. The independent and sequential Ca^{2+} binding to the EF-hands (in contrast to cooperative binding) suggests a molten globule or unstructured form of apoDREAM-C that lacks long range structural interaction between the EF-hands. Indeed, the NMR spectrum of apoDREAM-C (see below) exhibits very poor chemical shift dispersion in the amide proton region, consistent with an unstructured apo-protein.

Constitutive Mg^{2+} Binding at EF-2—The presence of physiological levels of Mg^{2+} (5 mM Mg^{2+}) had a profound affect on the ITC Ca^{2+} binding isotherms of wild-type and EF-hand mutants (Fig. 3*B*). The Ca^{2+} binding isotherm of wild-type in the presence of physiological Mg^{2+} was saturated with a Ca^{2+} binding stoichiometry of two, in contrast to a stoichiometry of three in the absence of Mg^{2+} (Fig. 3*A*). The Ca^{2+} binding isotherm of D150N in the presence of physiological Mg^{2+} looked remarkably similar to that of wild-type and was saturated with a Ca^{2+} binding stoichiometry of two. The Ca^{2+} binding isotherms of E186Q and E234Q in the presence of physiological Mg^{2+} both saturated with a Ca^{2+} binding stoichiometry of one. These results imply that Ca^{2+} does not bind to EF-2 in the presence of Mg^{2+} (Fig. 3*B*), suggesting that EF-2 binds constitutively to Mg^{2+} under physiological conditions (*i.e.* 5 mM Mg^{2+} and 0.1–100 μM Ca^{2+}). The presence of Asp-150 (instead of Glu) at the 12-position of the Ca^{2+} binding loop of EF-2 might explain the loss of Ca^{2+} selectivity by EF-2. A shorter side chain at the 12-position would energetically favor binding of Mg^{2+} over Ca^{2+} as has been seen in other EF-hand proteins (23). Constitutive Mg^{2+} binding at EF-2 might somehow mediate the binding of DREAM to DNA targets.

The wild-type Ca^{2+} binding isotherm obtained at physiological Mg^{2+} levels is not accurately represented as a linear combination of isotherms from single-site mutants (Fig. 3*B*). Therefore, EF-3 and EF-4 do not represent independent binding sites in this case, suggesting some type of cooperativity between the two sites induced by Mg^{2+}. Cooperative Ca^{2+} binding to EF-3 and EF-4 might also explain the U-shaped binding isotherm of wild-type (Fig. 3*B*). Mg^{2+} binding to DREAM-C stabilizes its tertiary structure (see below), which presumably should enhance structural interactions between EF-3 and EF-4 as seen in previous x-ray structures of NCS proteins (18, 19, 22). Notably, the recent x-ray structure of the DREAM homolog, KChIP1, shows Ca^{2+} bound only at EF-3 and EF-4. We suggest that cooperative Ca^{2+} binding to EF-3 and EF-4 is facilitated by extensive structural contacts between the two sites and may serve as a switch for controlling Ca^{2+} sensitive binding of DREAM-C to DNA targets.

DREAM-C Has a High Affinity Mg^{2+} Site—The affect of Mg^{2+} on the Ca^{2+} binding isotherm of DREAM-C (Fig. 3) prompted us to quantitate the Mg^{2+}-binding properties of DREAM using isothermal titration calorimetry (ITC). Titration of $MgCl_2$ into DREAM-C resulted in a two-phase binding isotherm for wild-type (Fig. 4) and each of the EF-hand mutants (data not shown). An exothermic phase at the beginning of the isotherm represents binding of a single Mg^{2+} followed by en-

dothermic binding of non-stoichiometric Mg^{2+} (*i.e.* 1 or more Mg^{2+} with $K_d >$ protein concentration used for ITC). Analysis of the binding isotherm using a "two sites" model (Microcal Origin software) revealed that DREAM-C has one Mg^{2+} site with relatively high affinity (dissociation constant of 13 μM and $\Delta H = -0.79$ kcal/mol), and two or more sites with much lower affinity (K_d in the millimolar range and $\Delta H = +3.97$ kcal/mol). Intrinsic Mg^{2+} binding to most proteins is usually entropically driven (30). The enthalpic binding of Mg^{2+} to DREAM-C suggests a possible Mg^{2+}-induced conformational change. NMR spectra of DREAM-C change quite dramatically upon the addition of saturating Mg^{2+} (see below), suggesting that Mg^{2+} binding stabilizes tertiary structure of DREAM-C.

Also noteworthy was our observation that each EF-hand mutant exhibited Mg^{2+} binding similar to that of wild-type. Apparently, the EF-hand mutation at the 12-position in our study does not impair Mg^{2+} binding like it does for Ca^{2+}. Different coordination numbers for Mg^{2+} and Ca^{2+} might explain their different binding behavior in this regard (33).

Mg^{2+}/Ca^{2+} Effects on Oligomerization of DREAM-C—Previous dynamic light scattering and size-exclusion chromatography (SEC) analysis of metal-free DREAM-C (apoDREAM-C) originally indicated a mixture of aggregated protein species in solution (10). The presence of 10 mM lauryldimethylamine oxide detergent increased the solubility of apoDREAM-C and stabilized the metal-free protein in a tetrameric state. The DREAM tetramer is believed to bind functionally to DNA response elements in the prodynorphin and c-*fos* genes (9). In our current SEC study (Fig. 5), we now determine that DREAM-C in the presence of physiological Mg^{2+} levels (5 mM $MgCl_2$ and absence of detergent or DNA) eluted with an apparent molecular mass of 30 kDa in solution, which is slightly higher than the mass calculated for a protein monomer (25 kDa). The slightly higher apparent molecular mass in solution (30 *versus* 25 kDa) might be attributed to a non-spherical shape factor or perhaps a small percentage of dimer formation and was independent of protein concentration below 0.4 mM. Dynamic light scattering analysis similarly revealed a monomeric hydrodynamic radius for Mg^{2+}-bound DREAM-C. These results suggest that Mg^{2+} binding to one or more EF-hands (Fig. 4) stabilizes the protein mainly in a monomeric state at protein concentrations below 0.4 mM. By contrast, Ca^{2+}-saturated DREAM-C in the presence of Mg^{2+} eluted with an apparent molecular mass of 50 kDa in solution (Fig. 5), indicating that the Ca^{2+}-bound protein forms a stable dimer even at very dilute protein concentrations (10). Similar calcium-sensitive hydrodynamic properties were observed for each of the EF-hand mutants (data not shown), suggesting that each mutant is structurally intact. In summary, DREAM-C appears to be a monomer under basal physiological conditions (5 mM Mg^{2+} and 100 nM Ca^{2+}) and forms a stable dimer at saturating Ca^{2+} levels. A similar Ca^{2+}-induced dimerization has been reported previously for other NCS proteins such as neurocalcin (21).

Mg^{2+} and Ca^{2+} Stabilizes Tertiary Structure of DREAM-C—NMR spectroscopy was used to probe protein conformational changes in DREAM-C induced by Mg^{2+} and/or Ca^{2+} binding (Fig. 6). The peaks in the ^1H-^{15}N HSQC NMR spectra represent main-chain and side-chain amide groups and provide a fingerprint of the overall protein conformation. The two-dimensional ^1H-^{15}H HSQC spectrum of apoDREAM-C exhibited poorly resolved and overlapping peaks with narrow chemical shift dispersion in the amide proton dimension (Fig. 6*A*). The number of observed peaks was far less than the expected number of amide groups, and the intensities of many peaks were quite weak perhaps due to exchange broadening caused by conformational

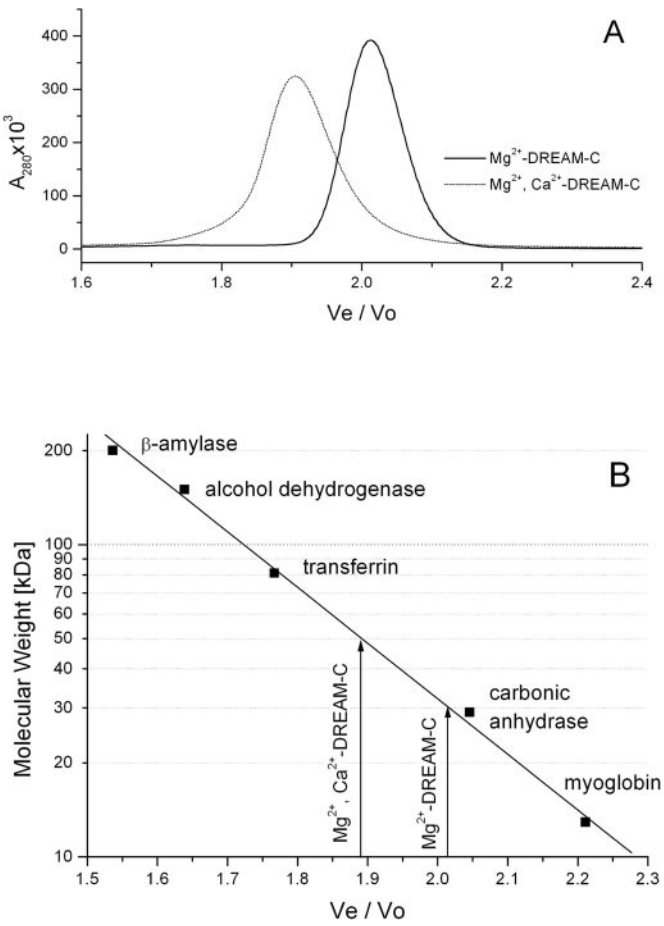

FIG. 5. **Molecular weight estimation of DREAM-C by size exclusion chromatography (SEC).** *A*, size exclusion chromatograms of Mg^{2+}- (*solid line*) and Mg^{2+}/Ca^{2+}-DREAM-C (*dotted line*). 100 μl of 200 μM protein solution were applied onto Superdex 200 HR (10/30) column (Amersham Biosciences) pre-equilibrated with the buffers containing 10 mM Hepes·NaOH (pH 7.6), 150 mM NaCl, 5 mM $MgCl_2$, 1 mM dithiothreitol, and 1 mM EGTA or 5 mM $CaCl_2$ for Mg^{2+}-DREAM-C and Ca^{2+}-DREAM-C, respectively. *B*, the standard curve for the molecular mass determination was created using β-amylase (200 kDa), alcohol dehydrogenase (150 kDa), transferrin (81 kDa), carbonic anhydrase (29 kDa), and myoglobin (17 kDa). Void volume of the column (*Vo*) was obtained as 7.81 ml using blue dextran (2000 kDa), and *Ve* is a volume of elution of each sample. *Arrows* indicate *Ve*/*Vo* values for Mg^{2+}- or Ca^{2+}-bound DREAM-C (50 μM). The molecular mass based on amino acid sequence of DREAM-C is 25 kDa.

heterogeneity. The poor chemical shift dispersion demonstrates that apoDREAM-C adopts an unstructured molten-globule state similar to that described for apo states of many other EF-hand proteins (30, 34, 35). Consistent with this interpretation is a lack of long range NOEs (particularly between aromatic and aliphatic resonances) in the homonuclear NOESY spectrum of apoDREAM-C (data not shown). However, circular dichroism analysis suggested that apoDREAM-C adopts a high degree of helical content, consistent with the formation of the four EF-hands, and the helical content did not change much upon binding Mg^{2+} and/or Ca^{2+}. Taken together, our structural studies indicate that apoDREAM-C adopts native secondary structure but is in a flexible molten-globule state.

The HSQC spectrum of DREAM-C changed dramatically upon the addition of saturating Mg^{2+} (Fig. 6*B*). Mg^{2+} caused a greater number of peaks to appear that were in general sharper than those of apoDREAM-C. Mg^{2+} binding to DREAM-C increased the NMR chemical shift dispersion and promoted long range NOEs in the NOESY spectrum (data not shown), demonstrating that Mg^{2+}-bound DREAM-C adopts at least some

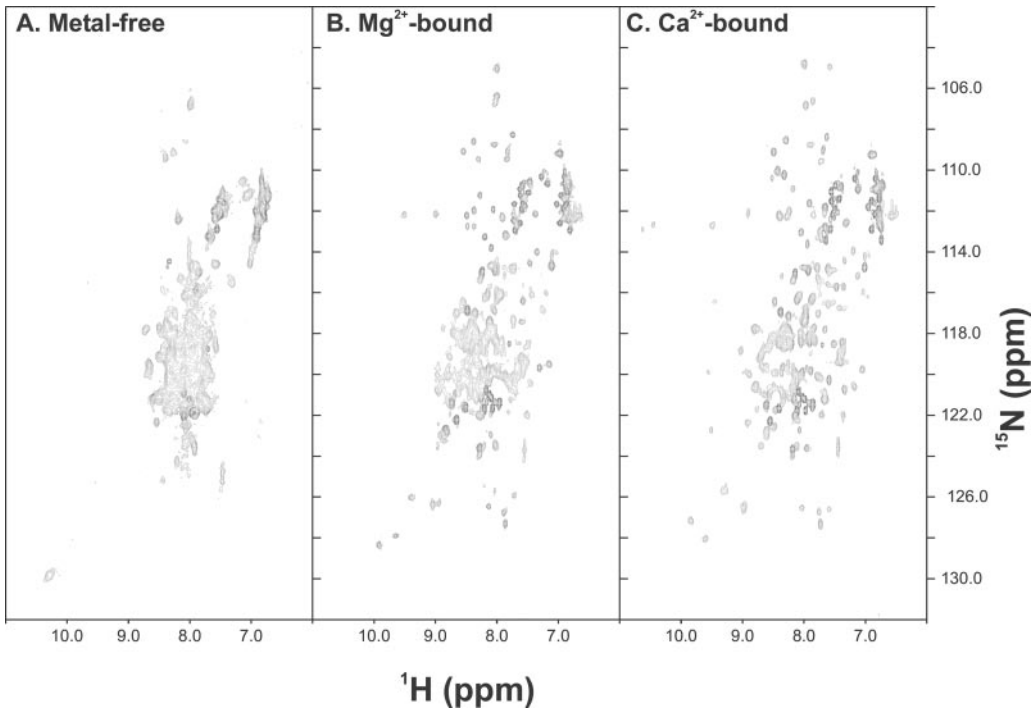

FIG. 6. **Two-dimensional ^{15}N-^{1}H HSQC NMR spectra of apo (*A*), Mg^{2+}-bound (*B*), and Ca^{2+}-bound (*C*) DREAM-C.** Each protein sample was uniformly labeled with nitrogen 15, and spectra were recorded at 600-MHz ^{1}H frequency.

stable tertiary structure in contrast to the metal-free protein. However, a number of peaks in the middle of the HSQC spectrum remained rather broad, suggesting that other parts of the Mg^{2+}-bound protein may not be structured or perhaps undergo conformational exchange. Pulsed-field gradient diffusion NMR studies (36) determined a hydrodynamic radius of 2.7 nm (corresponding to a spherical molecular mass of 34 kDa) for Mg^{2+}-bound DREAM-C under NMR conditions, which is slightly higher than that determined by SEC (Fig. 5). The apparent molecular mass for Mg^{2+}-bound DREAM-C observed by NMR increased monotonically as a function of protein concentration above 0.5 mM, consistent with low affinity dimer formation in the millimolar range.

The HSQC spectrum of DREAM-C changed even further upon the addition of two molar equivalents of Ca^{2+} (Fig. 6*C*). Significant spectral changes induced by adding Ca^{2+} to the Mg^{2+}-bound protein sample indicated that Ca^{2+}-induced conformational changes are distinct and separate from the Mg^{2+}-induced changes (Fig. 6, *B* and *C*). Two downfield-shifted peaks near 10.5 ppm are characteristic of conserved glycine residues at the 6-position of Ca^{2+}-occupied EF-hands, consistent with Ca^{2+} bound at EF-3 and EF-4. Additional unique peaks of Ca^{2+}-bound DREAM-C (*e.g.* near 9.5 ppm) represent amino acid residues in EF-3 or EF-4 stabilized structurally by Ca^{2+} binding. The HSQC spectrum of Ca^{2+}/Mg^{2+}-saturated DREAM-C exhibited variable peak intensities, suggesting exchange broadening perhaps associated with Ca^{2+}-induced dimerization (see Fig. 5). Pulsed-field gradient diffusion NMR studies determined a hydrodynamic radius of 3.2 nm, corresponding to a stable Ca^{2+}-bound protein dimer that persisted under a wide range of protein concentrations (0.05–1 mM).

DNA Binding by EF-hand Mutants versus Ca^{2+}—Electrophoresis mobility shift assays (EMSA) were performed on the EF-hand mutants to monitor their Ca^{2+}-sensitive binding to duplex oligonucleotide derived from the downstream response element (DRE) of the prodynorphin gene (Fig. 7). The EMSA binding data for wild-type and single-site EF-hand mutants look very similar, suggesting that each of the mutants bind to the DRE and are functionally intact. A typical EMSA for DREAM is shown in Fig. 7 and exhibits two shifted bands that represent different oligomeric species of DREAM bound to

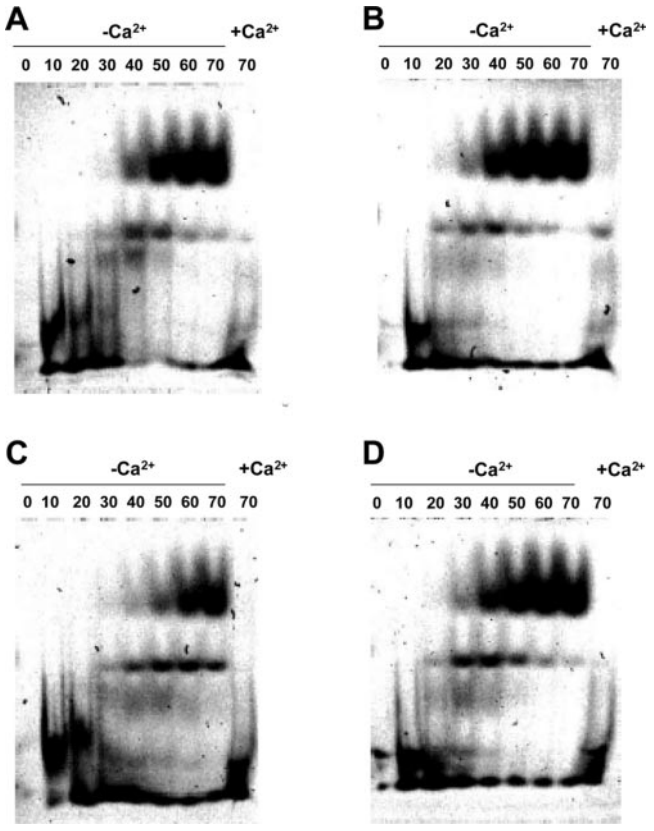

FIG. 7. **Electrophoretic mobility shift assay of DREAM-C/DRE interaction.** 5 nM Cy5 labeled DRE oligonucleotide in 10 mM HEPES, pH 7.9, 2 mM dithiothreitol, and 8 mM Mg^{2+} was incubated with 0–70 μM wild-type (*A*), D150N (*B*), E186Q (*C*), and E234Q (*D*) DREAM-C in the presence and absence of 10 mM Ca^{2+}.

DRE. The lower shifted band has variable intensity, is not sequence-specific, is less responsive to Ca^{2+}, and may represent DNA binding by the DREAM dimer or monomer. The uppermost band (believed to represent a DREAM tetramer) has been characterized previously to represent sequence-specific binding to DRE (9, 10), and we found in this study that this band requires saturating levels of Mg^{2+}. The Mg^{2+}-dependent DRE binding to D150N mutant suggests that this mutation does not impair high affinity Mg^{2+} binding at EF-2 (Fig. 4) perhaps needed for DRE binding. The EMSA shifted bands for wild-type and each of the EF-hand mutants (D150N, E186Q, and E234Q) disappear upon the addition of saturating Ca^{2+}, suggesting that the Ca^{2+}-bound forms of the EF-hand mutants (like wild-type) do not bind to DRE. In summary, Mg^{2+} is required for sequence-specific binding to DRE and Ca^{2+} binding at either EF-3 or EF-4 is sufficient to abolish DNA binding.

Mechanism of Ca^{2+}-sensitive DNA Binding—In this study, we showed that Mg^{2+} is essential for DNA binding by DREAM-C; EF-2 binds Mg^{2+} (and not Ca^{2+}) under physiological conditions; EF-3 and EF-4 bind functionally to Ca^{2+} and induce protein dimerization; and binding of a single Ca^{2+} at either EF-3 or EF-4 is sufficient to drive protein conformational changes responsible for abolishing DNA binding at high Ca^{2+}. What do these structural facts imply about the mechanism of Ca^{2+}-sensitive DNA binding by DREAM? One clear implication is that Mg^{2+} binding at EF-2 may be important for promoting DREAM binding to DNA targets. The bound Mg^{2+} at EF-2 could structurally bridge DREAM to DNA, perhaps by forming an axial coordinate covalent bond with a phosphoryl oxygen atom from DNA. Previous x-ray structures have illustrated many examples where divalent cations bridge phosphate groups of DNA with various DNA-binding proteins (37–39). A similar type of metal ion bridge serves to link membrane proteins (*e.g.* C2 domains and annexin V) with the phosphoryl oxygen from lipid head groups (40, 41).

A second implication of this study is that Ca^{2+} binding at EF-3 and EF-4 promotes protein dimerization that somehow disrupts DNA binding by DREAM. In the Ca^{2+}-bound protein, residues at the dimer interface (perhaps in EF-3 or EF-4) might sterically block residues of the Ca^{2+}-free protein that contact DNA. The recent x-ray structure of a closely related DREAM-like protein, KChIP1, shows a dimeric structure for the Ca^{2+}-bound protein with intermolecular contacts between a hydrophobic groove (formed by EF-1 and EF-2) and a C-terminal helix adjacent to EF-4 (19). The C-terminal helix of KChIP1 (residues 205–215) forms extensive *intra*molecular contacts with both EF-3 and EF-4, whereas the opposite face of the C-terminal helix forms *inter*molecular contacts with EF-1 and EF-2. It is plausible that Ca^{2+}-induced conformational changes in either EF-3 or EF-4 would alter the disposition of the C-terminal helix and promote intermolecular contact with EF-1 and EF-2. An intriguing hypothesis follows that Ca^{2+}-induced dimerization might sterically alter the structure of EF-2 (due to an interaction with the C-terminal helix) and thereby disrupt an Mg^{2+} ion bridge with DNA. In the future, we plan to determine the atomic-level structure of DREAM-DNA complex and Ca^{2+}-induced conformational changes to more rigorously understand the structural basis of Ca^{2+}-sensitive DNA binding by DREAM.

Acknowledgments—We thank Fred Schwarz for assistance with the ITC experiments, Fenhong Song for oligonucleotide DNA synthesis, and Nese Sari for help with NMR experiments.

REFERENCES

1. Buxbaum, J. D., Choi, E. K., Luo, Y., Lilliehook, C., Crowley, A. C., Merriam, D. E., and Wasco, W. (1998) *Nat. Med.* **4,** 1177–1181
2. An, W. F., Bowlby, M. R., Betty, M., Cao, J., Ling, H. P., Mendoza, G., Hinson, J. W., Mattsson, K. I., Strassle, B. W., Trimmer, J. S., and Rhodes, K. J. (2000) *Nature* **403,** 553–556
3. Vogt, B. A. (2002) *N. Engl. J. Med.* **347,** 362–364
4. Costigan, M., and Woolf, C. J. (2002) *Cell* **108,** 297–300
5. Buxbaum, J. D. (2004) *Biochem. Biophys. Res. Commun.* **322,** 1104–1144
6. Zaidi, N. F., Thomson, E. E., Choi, E. K., Buxbaum, J. D., and Wasco, W. (2004) *J. Neurochem.* **89,** 593–601
7. Carrion, A. M., Mellstrom, B., and Naranjo, J. R. (1998) *Mol. Cell. Biol.* **18,** 6921–6929
8. Ledo, F., Link, W. A., Carrion, A. M., Echeverria, V., Mellstrom, B., and Naranjo, J. R. (2000) *Biochim. Biophys. Acta* **1498,** 162–168
9. Carrion, A. M., Link, W. A., Ledo, F., Mellstrom, B., and Naranjo, J. R. (1999) *Nature* **398,** 80–84
10. Osawa, M., Tong, K. I., Lilliehook, C., Wasco, W., Buxbaum, J. D., Cheng, H. Y., Penninger, J. M., Ikura, M., and Ames, J. B. (2001) *J. Biol. Chem.* **276,** 41005–41013
11. Ledo, F., Kremer, L., Mellstrom, B., and Naranjo, J. R. (2002) *EMBO J.* **21,** 4583–4592
12. Cheng, H. Y., Pitcher, G. M., Laviolette, S. R., Whishaw, I. Q., Tong, K. I., Ikura, M., Salter, M. W., and Penninger, J. M. (2002) *Cell* **108,** 31–43
13. Lilliehook, C., Bozdagi, O., Yao, J., Gomez, M., Zaidi, N. F., Wasco, W., Gandy, S., and Buxbaum, J. D. (2003) *J. Neurosci.* **23,** 9097–9106
14. Moncrief, N. D., Kretsinger, R. H., and Goodman, M. (1990) *J. Mol. Evol.* **30,** 522–562
15. Ikura, M. (1996) *Trends Biochem. Sci.* **21,** 14–17
16. Ames, J. B., Tanaka, T., Stryer, L., and Ikura, M. (1996) *Curr. Opin. Struct. Biol.* **6,** 432–438
17. Burgoyne, R. D., and Weiss, J. L. (2001) *Biochem. J.* **353,** 1–12
18. Flaherty, K. M., Zozulya, S., Stryer, L., and McKay, D. B. (1993) *Cell* **75,** 709–716
19. Zhou, W., Qian, Y., Kunjilwar, K., Pfaffinger, P. J., and Choe, S. (2004) *Neuron* **41,** 573–586
20. Scannevin, R. H., Wang, K., Jow, F., Megules, J., Kopsco, D. C., Edris, W., Carroll, K. C., Lu, Q., Xu, W., Xu, Z., Katz, A. H., Olland, S., Bowlby, M. R., Chanda, P., and Rhodes, K. J. (2004) *Neuron* **41,** 587–598
21. Vijay-Kumar, S., and Kumar, V. D. (1999) *Nat. Struct. Biol.* **6,** 80–88
22. Bourne, Y., Dannenberg, J., Pollmann, V. V., Marchot, P., and Pongs, O. (2001) *J. Biol. Chem.* **276,** 11949–11955
23. da Silva, A. C., Kendrick-Jones, J., and Reinach, J. C. (1995) *J. Biol. Chem.* **270,** 6773–6778
24. Craig, T. A., Benson, L. M., Venyaminov, S. Y., Klimtchuk, E. S., Bajzer, Z., Prendergast, F. G., Naylor, S., and Kumar, R. (2002) *J. Biol. Chem.* **277,** 10955–10966
25. Brocard, J. B., Rajdev, S., and Reynolds, I. J. (1993) *Neuron* **11,** 751–757
26. Cox, J. A., Durussel, I., Comte, M., Nef, S., Nef, P., Lenz, S. E., and Gundelfinger, E. D. (1994) *J. Biol. Chem.* **269,** 32807–32813
27. Peshenko, I. V., and Dizhoor, A. M. (2004) *J. Biol. Chem.* **279,** 16903–16906
28. Wiseman, T., Williston, S., Brandts, J. F., and Lin, L. N. (1989) *Anal. Biochem.* **179,** 131–137
29. Schwarz, F. P., Puri, K. D., Bhat, R. G., and Surolia, A. (1993) *J. Biol. Chem.* **268,** 7668–7677
30. Yamniuk, A. P., Nguyen, L. T., Hoang, T. T., and Vogel, H. J. (2004) *Biochemistry* **43,** 2558–2568
31. Ames, J. B., Hamasaki, N., and Molchanova, T. (2002) *Biochemistry* **41,** 5776–5787
32. Maune, J. F., Klee, C. B., and Beckingham, K. (1992) *J. Biol. Chem.* **267,** 5286–5295
33. Cates, M. S., Teodoro, M. L., and Phillips, G. N. (2002) *Biophys. J.* **82,** 1133–1146
34. Ames, J. B., Dizhoor, A. M., Ikura, M., Palczewski, K., and Stryer, L. (1999) *J. Biol. Chem.* **274,** 19329–19337
35. Ames, J. B., Hendricks, K. B., Strahl, T., Huttner, I. G., Hamasaki, N., and Thorner, J. (2000) *Biochemistry* **39,** 12149–12161
36. Altieri, A. S., Hinton, D. P., and Byrd, R. A. (1995) *J. Am. Chem. Soc.* **117,** 7566–7567
37. Brautigam, C. A., Sun, S., Piccirilli, J. A., and Steitz, T. A. (1999) *Biochemistry* **38,** 696–704
38. Deibert, M., Grazulis, S., Sasnauskas, G., Siksnys, V., and Huber, R. (2000) *Nat. Struct. Biol.* **7,** 792–799
39. Subirana, J. A., and Soler-Lopez, M. (2003) *Annu. Rev. Biophys. Biomol. Struct.* **32,** 27–45
40. Ochoa, W. F., Corbalan-Garcia, S., Eritja, R., Rodriguez-Alfaro, J. A., Gomez-Fernandez, J. C., Fita, I., and Verdaguer, N. (2002) *J. Mol. Biol.* **320,** 277–291
41. Swairjo, M. A., Concha, N. O., Kaetzel, M. A., Dedman, J. R., and Seaton, B. A. (1995) *Nat. Struct. Biol.* **2,** 968–974